Computer simulation studies of anisotropic systems XIV. Binary mixtures of liquid crystals

R. Hashim[a]; G. R. Luckhurst[a]; S. Romano[ab]

[a] Department of Chemistry, The University, Southampton, England [b] Department of Physics, The University and GNSM-CNR, Pavia, PV, Italy

PLEASE SCROLL DOWN FOR ARTICLE

Computer simulation studies of anisotropic systems
XIV. Binary mixtures of liquid crystals

by R. HASHIM, G. R. LUCKHURST and S. ROMANO†

Department of Chemistry, The University, Southampton, SO9 5NH, England

We have simulated the behaviour of a model, binary mixture of nematogens composed of cylindrically symmetric particles using the Monte Carlo technique. The characteristics of the model mixture were chosen to be in accord with most of the assumptions made in the Humphries–James–Luckhurst theory of liquid crystalline mixtures. The results of the simulation experiments allow us to test, for the first time, the validity of the molecular field approximation in this theory. In addition to the second rank long range orientational order parameters for both components of the mixture we have also determined certain orientational pair correlation functions. These enable us to investigate the ability of one component to enhance the order of the other component or the same component in its vicinity.

1. Introduction

Mixtures of liquid crystals are of fundamental interest and of technological importance. Thus the nematogenic materials employed in electro-optic displays are multicomponent mixtures whose nature and composition are selected to achieve particular display characteristics [1]. For example, the liquid crystalline range is enhanced by the addition of nematogens with high nematic–isotropic transition temperatures, such as the 4-n-alkyl-4″-cyanoterphenyls, to materials with lower transitions such as the corresponding cyanobiphenyls. Solutions of pleochroic dyes in a nematogenic solvent are also of potential importance in display technology [2]. Liquid crystalline mixtures are of fundamental interest because their properties provide a unique insight into the anisotropic interactions between unlike species. An understanding of these properties requires a molecular theory of liquid crystalline mixtures, in addition such theories are also of value in the design of mixtures for display devices.

One of the earliest theories for multicomponent mixtures, formed from cylindrically symmetric particles, was developed by Humphries, James and Luckhurst based on the molecular field approximation [3]. This gave the potential of mean torque for component A in a binary liquid crystalline mixture as

$$U_A(\cos\beta) = -\{(1 - x)\bar{u}_2^{AA}\bar{P}_2^A + x\bar{u}_2^{AB}\bar{P}_2^B\}P_2(\cos\beta) \qquad (1)$$

and for the other component

$$U_B(\cos\beta) = -\{(1 - x)\bar{u}_2^{AB}\bar{P}_2^A + x\bar{u}_2^{BB}\bar{P}_2^B\}P_2(\cos\beta), \qquad (2)$$

where $P_2(\cos\beta)$ is the second Legendre polynomial and β is the angle made by the molecular symmetry axis of a particular species with the director. The second rank

orientational order parameters for components A and B are written as $\bar{P}_2^A$ and $\bar{P}_2^B$, respectively. The mole fraction of component B is denoted by x, $\bar{u}_2^{AA}$ is an average strength parameter for anisotropic interactions between species A and $\bar{u}_2^{AB}$ is that for interactions between unlike species. The particular composition dependence for the potentials of mean torque results from the assumption of random mixing in the solution. The theory further assumes the Berthelot rule

$$\bar{u}_2^{AB} = (\bar{u}_2^{AA} \bar{u}_2^{BB})^{1/2} \tag{3}$$

to relate the mixed interaction parameter to those for the pure components. With this assumption the nematic–isotropic transition temperature for the mixture was found to be linearly dependent on those of the components

$$T_{NI}^M = (1 - x) T_{NI}^A + x T_{NI}^B. \tag{4}$$

Here the transition temperatures T_{NI}^A and T_{NI}^B are related to the interaction parameters by, for example, [4]

$$T_{NI}^A = 0 \cdot 2203 \, \bar{u}_2^{AA}/k. \tag{5}$$

This simple result for T_{NI}^M was obtained by ignoring the possibility of separation into nematic and isotropic phases at the transition, although this must occur in practice because the nematic–isotropic transition is first order. The theory has been extended to allow for phase separation [5, 6] but for many mixtures of nematogens the width of the biphasic region is very small. The Humphries–James–Luckhurst theory may also be used to predict the orientational order parameters for the individual components as a function of either composition or temperature. For example, at a fixed temperature the composition dependence of the two order parameters in a binary mixture is found to be similar with an essentially constant difference between them, the component with the higher transition having the larger order parameter [7]. The compositionally weighted average

$$\bar{P}_2^M = (1 - x) \bar{P}_2^A + x \bar{P}_2^B, \tag{6}$$

which is usually measured in experimental studies of mixtures is found [7] to vary in a manner predicted by the analogous theory for single component systems proposed by Maier and Saupe [4].

There have been relatively few tests of the various theoretical predictions, although such evidence that is available appears to support the theory [3, 8, 9]. None the less it would be of considerable value to have more detailed experimental results which would allow an evaluation of the reliability of specific approximations made in developing the theory. Thus the mixture should be composed of rigid, cylindrically symmetric particles, the anisotropic interactions should be of second rank, the mixing should be random, separate phases should not be formed at the nematic–isotropic transition and the volume of transition should be zero. Clearly such demanding constraints cannot be met by real nematogenic mixtures whose component molecules are flexible and of low symmetry, in addition the nature of the anisotropic interactions are unknown. We have therefore undertaken a computer simulation study of a model binary nematogenic mixture. This has the major advantage that all of the constraints can be satisfied which allows us to provide a unique test of the use of the molecular field approximation for nematogenic mixtures. The precise nature of the model is described in the following section. In §3 the Monte Carlo method used to study the mixture is outlined and the properties which are evaluated by the simulation are

described. The results of the computations are given in §4 where they are compared with the predictions of the Humphries–James–Luckhurst theory.

2. The model nematogenic mixture

We take as a model for the pure nematogenic components that proposed and investigated by Luckhurst, Romano and Simpson [10]. In this the cylindrically symmetric particles are confined to the sites of a face centred cubic lattice; the practical advantages and conceptual disadvantages of using lattice models for liquid crystals have been discussed elsewhere [11]. The anisotropic interactions are restricted to nearest neighbours and for these take the form

$$U_{ij} = -\varepsilon P_2(\cos \beta_{ij}), \qquad (7)$$

where ε is a positive constant and β_{ij} is the angle between the symmetry axes of particles i and j. This system exhibits a weak, first order phase transition between orientationally ordered and disordered phases when the scaled temperature T^* ($\equiv kT/\varepsilon$) is equal to $2\cdot43 \pm 0\cdot03$. The second rank order parameter, $\bar{P}_2$, at the transition is $0\cdot31 \pm 0\cdot03$ and the entropy of transition, $\Delta S/R$, is $0\cdot04 \pm 0\cdot02$; these values are typical of those determined for real nematics.

The extension of this model to a binary mixture necessitates the introduction of three pair potentials each with a particular interaction parameter ε_{AA}, ε_{BB} and ε_{AB}. However to simplify the computations we have used such a low concentration of component B that the probability of finding them as nearest neighbours is negligible and so ε_{BB} does not enter the calculation. Low concentrations are certainly compatible with that of a dye in a nematogenic solution and also that of the nematogens added to increase the nematic–isotropic transition of a mixture. As the concentration of component B is small we shall refer to it as the solute and to A as the solvent. The solute is placed at random on the lattice sites with the additional constraint that no two are nearest neighbours. This particular distribution remains unchanged during the simulation experiment and so phase separation at the transition cannot occur. We have shown for similar mixtures but with biaxial solutes that the results of the simulation are independent of the particular random distribution chosen for the solute [12].

3. The Monte Carlo simulations

We have employed the standard Monte Carlo technique with periodic boundary conditions, as introduced by Metropolis *et al.* [13]. The use of this simulation procedure in the study of model liquid crystals is described in detail elsewhere [10, 11] and so here we concentrate on those new features which result from the presence of two components.

The random distribution of the solute particles on the lattice was achieved in the following way. The N sites of the face centred cubic lattice were labelled with the integers 1 to N. The site for the first solute was chosen by generating a random number uniformly distributed in the range 0–1 and then converting it to an integer between 1 and N. The remaining solutes were allocated to lattice sites in the same manner but now the location of each new solute was checked to ensure that it was not adjacent to another solute. If it was then the location was rejected and a new site generated. This procedure was repeated until all solute particles had been assigned to the lattice.

The orientations of solute and solvent particles were stored as the unit vectors for their symmetry axes in the laboratory frame. These orientations were changed using the scheme proposed by Barker and Watts [14]. The two components were assigned different maximum displacements, Δ_A and Δ_B, in this scheme so that the acceptance : rejection ratios for solute and solvent may be kept at their optimum value of unity. It was not necessary to sample the solvent particles preferentially because the solute concentration was such that there are as many solvent particles adjacent to a solute as are not [15].

The properties evaluated by the simulations were the total scaled internal energy per particle, $\bar{U}^*$ ($\equiv \bar{U}/N\varepsilon_{AA}$) together with the internal energy associated with the interaction between solvent molecules alone, $\bar{U}^*_{AA}$ and between solute and solvent $\bar{U}^*_{AB}$. These particular properties were calculated because as we shall see for a lattice model with nearest neighbour interactions they are directly related to the short range orientational correlations. The heat capacity per particle, C^*_v, was determined both by numerical differentiation of the total internal energy with respect to temperature and from the fluctuations in the total internal energy

$$C^*_v = N\{\overline{\bar{U}^{*2}} - (\bar{U}^*)^2\}/T^{*2}, \tag{8}$$

where the scaled temperature T^* is kT/ε_{AA}. The observed divergence in C^*_v is used to locate the nematic–isotropic transition and hence to determine the transition temperature.

The orientational structure of the mixture was studied through the orientational correlation functions $G^{AA}_2(r^*)$, $G^{AA}_4(r^*)$ and $G^{AB}_2(r^*)$; here r^* is the scaled separation (r/a) between molecules of the particular species where $\sqrt{2}\,a$ is the lattice spacing. The functions are defined, for example, by

$$G^{AB}_2(r^*) = \overline{P_2\{\cos\beta_{AB}(r^*)\}}, \tag{9}$$

where $\beta_{AB}(r^*)$ is the angle between the symmetry axes of a solvent and a solute particle separated by r^*. For nearest neighbour separations ($r^* = 1$) the correlation functions are equal to the short range order parameters [11], for example,

$$G^{AA}_2(1) = \sigma^{AA}_2. \tag{10}$$

These order parameters are directly proportional to the appropriate internal energy for lattice models with interactions restricted to nearest neighbours, thus for the solvent,

$$\bar{U}^*_{AA} = -z\sigma^{AA}_2/2, \tag{11}$$

where z is the coordination number [11]. The fourth rank angular correlation function for the solvent was calculated because it provides a route to the fourth rank long range order parameter $\bar{P}^A_4$. In the limit of large separations the orientational correlations are lost and so

$$\lim_{r^* \to \infty} G^{AA}_4(r^*) = (\bar{P}^A_4)^2. \tag{12}$$

The analogous second rank quantities $\bar{P}^A_2$ and $\bar{P}^B_2$ could be obtained in the same way but as this is particularly demanding of computer time we have adopted an alternative approach. The long range order parameter is defined by

$$\bar{P}_2 = \overline{P_2(\cos\beta)}, \tag{13}$$

where β is the angle made by the molecular symmetry axis with the director. During the course of the simulation the director fluctuates in the laboratory frame but it may be located by evaluating the Q tensor [16]

$$Q_{ab} = (\overline{3l_a l_b} - \delta_{ab})/2, \tag{14}$$

where l_a is the direction cosine of the molecular symmetry axis with the laboratory a axis. The largest eigenvalue of $\mathbf{Q}$ gives the order parameter $\bar{P}_2$ and the components of the eigenvector associated with this are the direction cosines of the director in the laboratory frame [11, 16]. In principle the Q tensor could be diagonalized for every configuration during the production run and the largest eigenvalue averaged. In practice it is more economic in computer resources, first to average $\mathbf{Q}$ over many configurations, the number being restricted only to ensure that the director orientation does not change. The averaged Q tensor is then diagonalized and the largest eigenvector averaged over the production run.

In Monte Carlo simulations of dilute nematogenic solutions this procedure could be used to obtain the order parameter for the solvent but not for the solute because the number of solute particles is too small to locate the director accurately. We have therefore adopted the following scheme which was devised originally for our study of biaxial solutes [12]. We define a total Q tensor for the mixture by taking a linear combination of the Q tensors for the components

$$\mathbf{Q}^M = (1 - x)\mathbf{Q}^A + x\mathbf{Q}^B. \tag{15}$$

The eigenvector of $\mathbf{Q}^M$ associated with its largest eigenvalue is used to define the director orientation; this definition based on the total Q tensor stems from the fact that the director is a property of the mixture and not simply one of its components. The orthogonal matrix $\mathbf{R}$ which diagonalizes $\mathbf{Q}^M$ is then used to transform $\mathbf{Q}^A$ and $\mathbf{Q}^B$ to the director frame. The largest diagonal elements of $\mathbf{R}^{-1}\mathbf{Q}^A\mathbf{R}$ and $\mathbf{R}^{-1}\mathbf{Q}^B\mathbf{R}$ are averaged over the production run and these averages are identified as the second rank order parameters $\bar{P}_2^A$ and $\bar{P}_2^B$ for the solvent and solute, respectively.

We turn now to the computational details. The mixture contained a total of 500 particles which were placed on the sites of a cube of $5 \times 5 \times 5$ face centred unit cells. Of these, 25 sites were occupied by solutes corresponding to a mole fraction, x, of 0.05. The solute was taken to be more anisotropic than the solvent and this is reflected by the mixed interaction ε_{AB} which is twice that for the solvent ε_{AA}; thus

$$\varepsilon_{AB} = 2\varepsilon_{AA} \tag{16}$$

and so according to the Berthelot combining rule the interaction parameter for the pure solute is

$$\varepsilon_{BB} = 4\varepsilon_{AA}. \tag{17}$$

In consequence the nematic–isotropic transition temperature for the solute would be four times that for the solvent. The mixture was studied over the scaled temperature range from 1.4 to 3.5 which encompasses both ordered and disordered phases. The first configuration had complete orientational order; this was equilibrated at a scaled temperature of 0.5 for 2000 cycles where one cycle consisted of 500 configurations or attempted moves. The temperature was then increased to 1.0 and the system was further equilibrated for 4000 cycles. Finally the scaled temperature was set equal to 1.4 which was the first of the series. The mixture was equilibrated for 8000 cycles and the production run consisted of 5000 cycles. The starting configurations for higher

temperatures in the series were taken as the last configuration from the equilibration stage of the preceding lower temperature. With this choice the production stage for a given temperature as well as the equilibration stage for the next may be started at the same time, which is of some benefit. The equilibration and production runs again consisted of 8000 and 5000 cycles respectively except in the vicinity of the phase transition where the lengths of these runs were doubled. Unlike the other properties the pair correlation functions were calculated once for each cycle, using all pairs of particles, and then averaged over the production run. Finally we note that the optimum value for the maximum displacement of the solvent, Δ_A, was found to be approximately twice that of the solute Δ_B, which is in accord with the greater anisotropy of the solute–solvent interaction.

4. Results and discussion

We begin with the heat capacity, C_v^*, whose temperature dependence is shown in figure 1. The results for C_v^*, were calculated from the temperature derivative of the total internal energy (●) and from the fluctuations in the internal energy (□); the agreement between these two sets of results is seen to be very good. Also included in figure 1 is the temperature dependence of the heat capacity for the pure solvent [10]. The heat capacities for both systems are observed to diverge, as expected for first order phase transitions, although the divergence shown by the mixture is not so marked as that found for the pure solvent. The transition temperature of the mixture is estimated to be 2.73 ± 0.03 from C_v^* which is significantly greater than T_{NI}^* of 2.43 ± 0.03 found for the pure solvent [10]. Such an increase is to be anticipated because of the greater anisotropy of the solute and can be predicted from the Humphries–James–Luckhurst theory [3]. However the molecular field approximation used in this theory is known to overestimate the orientational order and hence the nematic–isotropic transition temperature. Thus for the pure solvent T_{NI}^* is predicted to be 2.643 corresponding to an overestimate of about 8 per cent [10]. It is to be expected therefore that T_{NI}^{M*} obtained from equation (4) for T_{NI}^* of the mixture with the theoretical transition temperatures will also be too large and this is indeed the
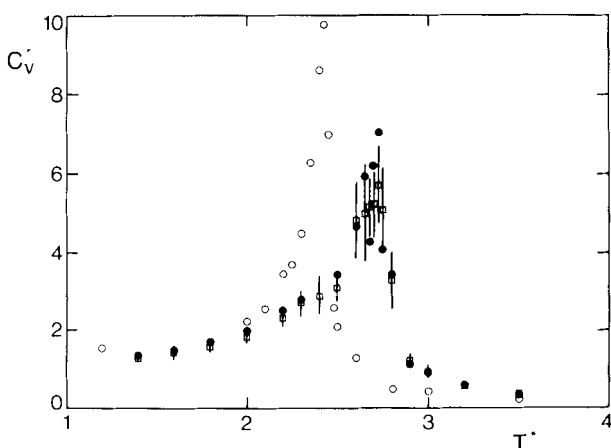

Figure 1.   The dependence of the scaled heat capacity per particle, C_v^*, on the scaled temperature, T^*, for the pure solvent (○) and for the mixture, calculated from the fluctuations in the internal energy (□) and its temperature derivative (●).

case, for T_{NI}^{M*} is found to be 3·038. We could, however, predict the transition temperature for the mixture from equation (4) but with the true transition temperature for the two components. T_{NI}^{A*} is 2·43 and since ε_{BB} is four times ε_{AA} (cf. equation (17)) T_{NI}^{B*} for the solute should be 9·72 which gives the transition temperature for the mixture as 2·79 $\pm$ 0·03 in good agreement with the value we have determined.

Strictly, equation (4) is not valid for the mixture which we have studied because solute–solute interactions are excluded; in consequence the potential of mean torque for the solute is given by

$$U_B(\cos \beta) = -\bar{u}_2^{AB} \bar{P}_2^A P_2(\cos \beta) \tag{18}$$

and not the expression contained in equation (2), but the solvent potential given in equation (1) still holds. However, for the low solute concentration employed in the simulation experiments there is little difference between the solute potential of mean torque in equations (2) and (18); the T_{NI}^* predicted by equation (4) should not therefore be seriously in error. None the less we have calculated the transition temperature for the mixture studied in the simulation with its pseudo-random solute distribution, using the correct potential for the solute. To obtain T_{NI}^M we require the difference in the orientational Helmholtz free energy, per particle, between the nematic and isotropic phases for the mixture, this is

$$\begin{aligned} \Delta A &= (1 - x)^2 \bar{u}_2^{AA} \bar{P}_2^{A2}/2 + x(2 - x)\bar{u}_2^{AB} \bar{P}_2^A \bar{P}_2^B/2 \\ &\quad - (1 - x)kT\ln(Z_A/2) - xkT\ln(Z_B/2). \end{aligned} \tag{19}$$

Here the orientational partition functions for the solute and solvent are given, for example, by

$$Z_A = \int \exp\{ - U^A(\cos \beta)/kT\} \sin \beta \, d\beta. \tag{20}$$

At the nematic–isotropic transition ΔA vanishes and for the mixture whose properties we have simulated this is found to occur when

$$T_{NI}^M = 0·2472 \bar{u}_2^{AA}/k. \tag{21}$$

The interaction parameter $\bar{u}_2^{AA}$ is related to the transition temperature for the pure solvent via equation (5); using the value for T_{NI}^{A*} of 2·43 obtained from the Monte Carlo simulation of the solvent [10] we find the scaled transition temperature for the mixture to be 2·73. This result is in exact agreement with the observed transition temperature for the mixture but as we had anticipated it does not differ greatly from the prediction based on the assumption of a perfectly random distribution for the solute and the solvent.

The long range, second rank orientational order parameters for the solvent, $\bar{P}_2^A$, (●) and for the solute, $\bar{P}_2^B$, (▲) are shown in figure 2 as a function of the reduced temperature, T^*/T_{NI}^{M*}. Use of a reduced temperature scale allows us to include the results for the pure solvent (○) and for these the reduced temperature is defined as T^*/T_{NI}^{A*}. All of the order parameters fall rapidly in the vicinity of the phase transition but do not vanish in the isotropic phase. This behaviour is characteristic of most simulation studies of model nematogens and results from the relatively small size of the system [11, 17] although it need not concern us here. The solute order parameter is seen to be considerably larger than that of the solvent in the mixture and this is to
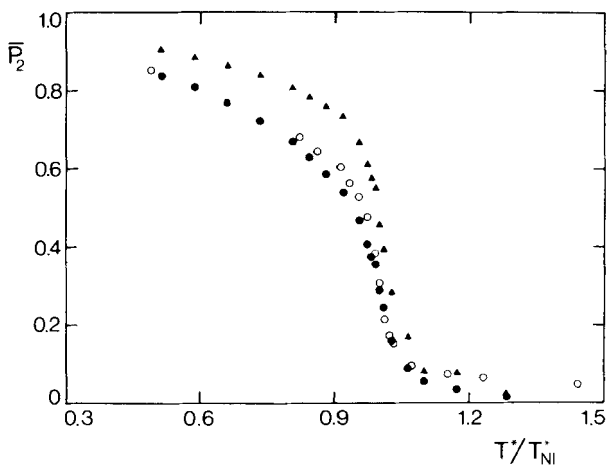
Figure 2.   The variation of the order parameter, $\bar{P}_2$, for the solute ($\blacktriangle$) and the solvent ($\bullet$) in the mixture as a function of the reduced temperature, T^*/T_{NI}^{M*}, together with that for the pure solvent (O) where T^*/T_{NI}^{A*} is the reduced temperature.

be expected given the greater anisotropy of the solute. The order parameter of the pure solvent is found to be slightly larger than that of the solvent in the mixture at the same reduced temperature. This difference is not so easily understood although it is in accord with predictions of the Humphries–James–Luckhurst theory [6, 9]. However, before we make a detailed comparison between the results of the simulations and the predictions of this theory we must see whether the angular dependence of the potential of mean torque is in accord with theory.

The singlet orientational distribution function, from which the potential of mean torque could be extracted, was not determined for either species from the Monte Carlo simulation, as this is particularly demanding in computer resources. Fortunately, it is possible to obtain some information about the potential from the second and fourth rank orientational order parameters which are available from the simulation, at least for the solvent. As we have seen the second rank order parameter, $\bar{P}_2^A$, is determined directly but $\bar{P}_4^A$ must be obtained from the large separation limit of the fourth rank orientational correlation function $G_4^{AA}(r^*)$ (cf. equation (12)). To ensure that this limit is reached for the size of system which we have been able to study we consider the behaviour of the second rank orientational correlation functions for the solvent with itself, $G_2^{AA}(r^*)$, and with the solute, $G_2^{AB}(r^*)$; these are shown in figures 3 (*a*), (*b*) respectively. We note that such pair correlation functions are forced to exhibit a minimum at a separation corresponding to half the dimension of the system by the periodic boundary conditions employed in the simulation. However we are able to see if the correlation functions have decayed to their limiting values because we have obtained the long range order parameters for the solute and solvent separately. The long range limits, of $(\bar{P}_2^A)^2$ and $\bar{P}_2^A \bar{P}_2^B$, are shown as the horizontal solid lines in figures 3 (*a*), (*b*), respectively and for scaled separations, r^*, greater than approximately 3 the correlation functions have clearly dropped to their limiting values. We may therefore use the fourth rank orientational correlation function, $G_4^{AA}(r^*)$, shown in figure 4, to determine the fourth rank order parameter, $\bar{P}_4^A$, for the solvent with some confidence; the results obtained from the limiting values of $G_4^{AA}(r^*)$ are listed in the table. We can now employ these, together with $\bar{P}_2^A$ determined at the same scaled
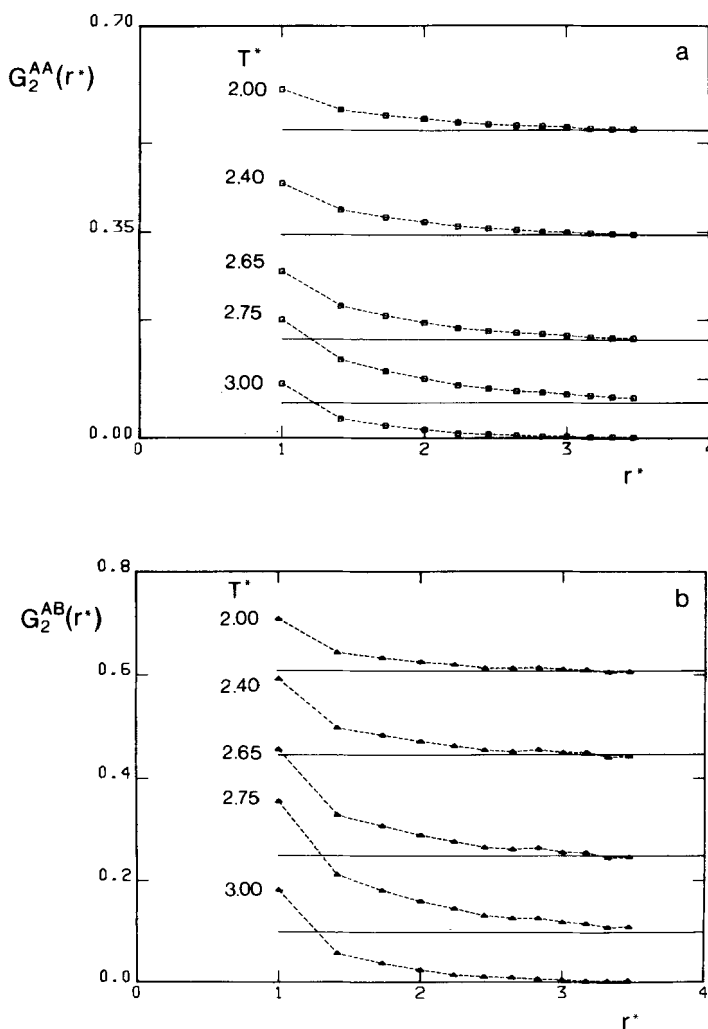
Figure 3. (*a*) The second rank orientational correlation function, $G_2^{AA}(r^*)$, for the solvent with itself, as a function of the scaled separation. (*b*) The dependence of the second rank orientational correlation function for the solvent with the solute, $G_2^{AB}(r^*)$, on the scaled separation, r^*. The solid lines in both figures show the large separation limits (*a*) $(\bar{P}_2^A)^2$ and (*b*) $\bar{P}_2^A \bar{P}_2^B$ calculated from the order parameters obtained directly from the simulation.

The fourth rank order parameter, $\bar{P}_4^A$, for the solvent determined from the limiting value of $G_4^{AA}(r^*)$ and predicted via equation (22) with a_A obtained from the observed $\bar{P}_2^A$.

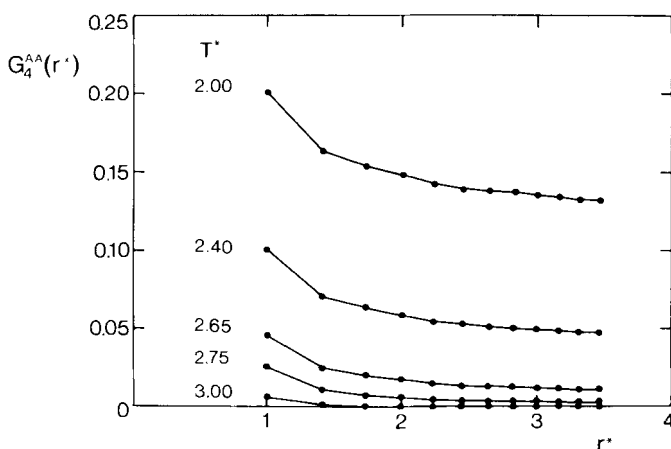| T^*	$\bar{P}_4^A$	
	Observed	Predicted
2·00	0·363	0·377
2·40	0·219	0·231
2·65	0·105	0·109
2·75	0·055	0·040

Figure 4. The fourth rank orientational correlation function, $G_4^{AA}(r^*)$, for the solvent with itself as a function of the scaled separation, r^*.

temperatures, to test the predicted form for the potential of mean torque. According to theory the orientational order parameters of rank L are given by

$$\bar{P}_L^A = Z_A^{-1} \int P_L(\cos \beta) \exp\{a_A P_2(\cos \beta)\} \sin \beta \, d\beta, \tag{22}$$

where the orientational partition function is

$$Z_A = \int \exp\{a_A P_2(\cos \beta)\} \sin \beta \, d\beta \tag{23}$$

and the coefficient a_A varies with temperature. However at a given temperature we can use the observed value of $\bar{P}_2^A$ to determine a_A this can then be employed to calculate $\bar{P}_4^A$ which may be compared with the simulation results. The predicted values of $\bar{P}_4^A$ are also given in the table and are seen to be in reasonably good agreement with those determined from the simulation, thus providing some confirmation for the angular variation of the potential of mean torque obtained from the theory.

Given this confirmation we may now compare the order parameters for both solute and solvent with those predicted by the Humphries–James–Luckhurst theory. As we have seen, the solvent order parameter, $\bar{P}_2^A$, can be used to determine the coefficient a_A in the potential of mean torque and according to theory this is given by

$$a_A = \{(1 - x)\bar{u}_2^{AA} \bar{P}_2^A + x\bar{u}_2^{AB} \bar{P}_2^B\}/kT \tag{24}$$

(cf. equation (1)). For the lattice model which we have studied the interaction parameters are predicted to be

$$\bar{u}_2^{AA} = z\varepsilon_{AA} \tag{25}$$

and

$$\bar{u}_2^{AB} = 2z\varepsilon_{AA}; \tag{26}$$

in consequence a plot of $a_A T^*$ against $\{(1 - x)\bar{P}_2^A + 2x\bar{P}_2^B\}$ should be linear through the origin with a slope equal to the coordination number, z. The results for such an analysis are shown in figure 5; the points clearly fall on a straight line which passes close to the origin. A least squares fit gives the slope of the line as 10.42 ± 0.05 which is not in complete agreement with the value required by theory of 12. Such a
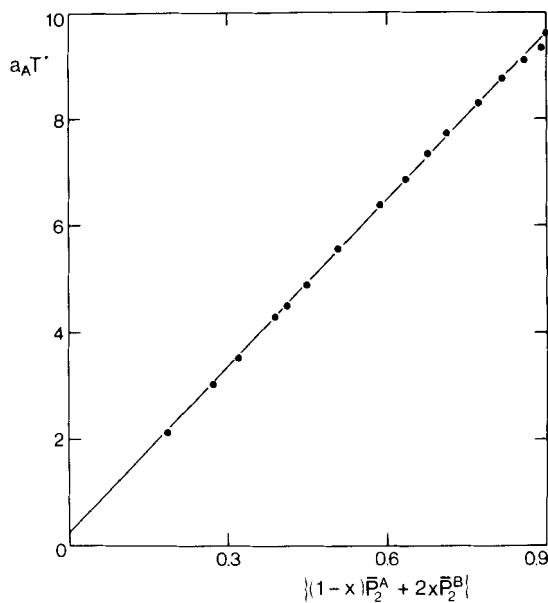
Figure 5.   The dependence of $a_A T^*$ for the solvent on the combination of solute and solvent order parameters $\{(1 - x)\bar{P}_A + 2x\bar{P}_B\}$; the straight line shows the best fit to the data.

discrepancy has also been observed for the Lebwohl–Lasher model nematogen where the effective coordination number, z_{eff}, is found to be 5.05 ± 0.02 in comparison with its true value of 6 and has been attributed to a failure of the molecular field approximation [18]. A similar analysis of the results obtained by Luckhurst, Romano and Simpson [10] for the pure solvent yield z_{eff} of 10.1 ± 0.1 in good agreement with the value found for the mixture.

The solute order parameter, $\bar{P}_2^B$, is given by an expression analogous to that in equation (22) but now the coefficient, a_B, in the potential of mean torque for the solute is given by

$$a_B T^* = 2z\bar{P}_2^A \tag{27}$$

(cf. equation (18)). As for the solvent a_B may be calculated from $\bar{P}_2^B$; $a_B T^*$ is indeed found to be linear in the solvent order parameter $\bar{P}_2^A$ and the straight line passes near to the origin. The effective coordination number determined from the slope is found to be 8.86 ± 0.05 which differs significantly from z found for the solvent, of 10.42 ± 0.05, as well as the true coordination number of 12. Clearly as the anisotropy in the solute–solvent interaction, ε_{AB}, approaches that for the solvent–solvent interaction, ε_{AA}, so the effective coordination number for the solute must tend to the value found for the solvent, which implies that z_{eff} depends on the anisotropy of the solute. In order to test this notion we have performed additional Monte Carlo simulations for which the anisotropy in the solute–solvent interaction was increased from $2\varepsilon_{AA}$ to $3\varepsilon_{AA}$ whilst keeping all other aspects of the model mixture the same. The system was not studied for as many temperatures nor for such a wide temperature range as the original model mixture. However we were able to determine the effective coordination number for the solvent and solute from their respective second rank orientational order parameters. Thus z_{eff} obtained from the solvent order parameter

was found to be $10 \cdot 0 \pm 0 \cdot 3$ whilst that from the solute is $7 \cdot 0 \pm 0 \cdot 3$. We see therefore that the increase in the anisotropy of the solute has no significant effect on the effective coordination number of the solvent but does reduce the value for the solute, as we had speculated. The molecular field approximation would appear to yield the angular dependence of the potentials of mean torque for both solute and solvent in good agreement with the simulation experiments. In addition the functional dependence of the coefficients, a_A and a_B, on the solvent and solute order parameters are also well predicted by the theory. However the effective coordination numbers for solute and solvent obtained from the simulation are not predicted by the molecular field approximation and for the solute the discrepancy increases with its anisotropy.

The molecular field approximation also fails to predict the correct behaviour of the orientational correlation functions, for according to this approximation $G_L(r^*)$ should be independent of the separation, r^*, and equal to its long range limit [4]. Thus for the solute–solvent second rank correlation function the approximation gives

$$G_2^{AB}(r^*) \;=\; \bar{P}_2^A \bar{P}_2^B. \tag{28}$$

From the results for $G_2^{AA}(r^*)$, $G_2^{AB}(r^*)$ and $G_4^{AA}(r^*)$ shown in figures 3 and 4 it is clear that for separations less than about 3 the correlation functions do depend on r^* and exhibit an increasing deviation from the long range limit as the separation decreases. In addition the orientational correlations are predicted to vanish in the isotropic phase, because the long range order parameters are zero, but clearly signficant correlations remain. Similar deviations from the molecular field approximation are observed [10, 11] for single component model nematogens and the failure of the approximation to predict the transition temperature as well as the entropy of transition has been attributed to these.

A highly anisotropic solute molecule is expected to be able to enhance the orientational order of less anisotropic solvent molecules in its vicinity to a greater extent than when they are near another solvent molecule. Indeed comparison of the results for $G_2^{AA}(r^*)$ with those for $G_2^{AB}(r^*)$, in figures 3 (a), (b) respectively, appears to support this expectation since at a given temperature $G_2^{AB}(r^*)$ is greater than $G_2^{AA}(r^*)$. However, part of this difference originates because the long range orientational order of the solute, $\bar{P}_2^B$, is higher than that for the solvent, $\bar{P}_2^A$. To compensate for this difference and to quantify the enhanced local ordering of the solvent by the solute we use the excess short range order parameter, $\Delta\sigma_2$ [10] which is defined, for example, by

$$\Delta\sigma_2^{AB} \;=\; \sigma_2^{AB} - \bar{P}_2^A \bar{P}_2^B. \tag{29}$$

The values for the short range order parameters, σ_2^{AA} and σ_2^{AB}, were determined from the solvent–solvent and solute–solvent contributions to the internal energy via equation (11). The results for $\Delta\sigma_2$ are shown in figure 6 as a function of the reduced temperature since this scale allows a comparison with the corresponding results for the pure solvent [10]. As we can see all three excess short range order parameters increase with increasing temperature and pass through a maximum at the nematic–isotropic transition which therefore corresponds to the temperature when the error in the molecular field approximation is greatest; if the approximation was exact $\Delta\sigma_2$ would vanish. The excess solute–solvent short range order parameter $\Delta\sigma_2^{AB}$ is clearly the largest and so confirms the expected greater ability of the solute to enhance the local solvent order in comparison with that of the solvent to order neighbouring solvent molecules. This ability of the highly anisotropic solute is of considerable interest for the interpretation of the ordering behaviour of liquid crystalline mixtures.
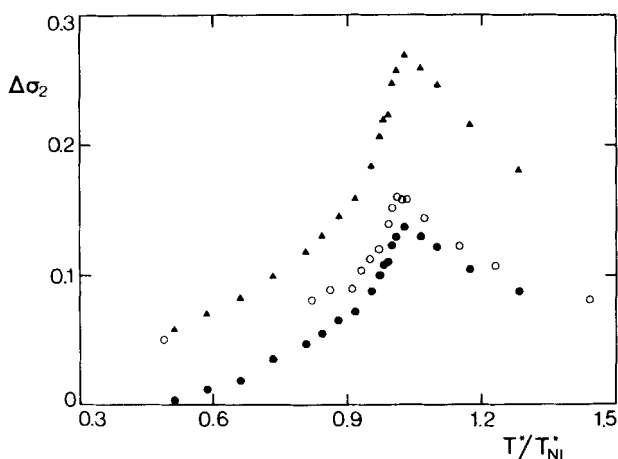
Figure 6. The excess short range order parameter $\Delta\sigma_2$ for solute with solvent ($\blacktriangle$) and for solvent with itself ($\bullet$) in the mixture as a function of the reduced temperature, T^*/T_{NI}^{M*}. The corresponding results, $\Delta\sigma_2^{AA}$, for the pure solvent as a function of T^*/T_{NI}^{A*} are shown as ($\bigcirc$).

For example, it may well be of relevance to systems such as proteins dissolved in membranes where the lipid in the vicinity of the protein is claimed to be more highly ordered than in the bulk [19], although this view is not universally accepted [20]. The results in figure 6 also reveal that the excess short range order, $\Delta\sigma_2^{AA}$, in the pure solvent is greater than for the mixture at the same reduced temperature. This significant difference is in accord with the slight depression of the long range order parameter $\bar{P}_2^A$ for the solvent by the addition of the solute. Such behaviour of $\bar{P}_2^A$ is certainly predicted by the Humphries–James–Luckhurst theory but this theory is quite unable to account for $\Delta\sigma_2$ and its variations. The short range order is available from cluster theories [21] and the theory of nematic disorder proposed by Faber [22] but although these have been developed for pure nematogens we are unaware of similar theories for mixtures.

References
[1] CLARK, M. G., HARRISON, K. J., and RAYNES, E. P., 1980, *Phys. Technol.*, **11**, 232.
[2] HEILMEIER, G. H., and ZANONI, C. A., 1968, *Appl. Phys. Lett.*, **13**, 91. WHITE, D. L., and TAYLOR, G. N., 1974, *J. appl. Phys.*, **45**, 4718.
[3] HUMPHRIES, R. L., JAMES, P. G., and LUCKHURST, G. R., 1971, *Symp. Faraday Soc.*, **5**, 107.
[4] See, for example, LUCKHURST, G. R., 1979, *The Molecular Physics of Liquid Crystals*, edited by G. R. Luckhurst and G. W. Gray (Academic Press), Chap. 4.
[5] See, for example, MARTIRE, D. E., 1979, *The Molecular Physics of Liquid Crystals*, edited by G. R. Luckhurst and G. W. Gray (Academic Press), Chap. 11.
[6] PALFFY-MUHORAY, P., DUNMUR, D. A., MILLER, W. H., and BALZARINI, D. A., 1984, *Liquid Crystals and Ordered Fluids*, Vol. 4, edited by A. C. Griffin and J. F. Johnson (Plenum Press), p. 615.

[7] LUCKHURST, G. R., 1971, *Symp. Faraday Soc.,* **5**, 135.

[8] LUCKHURST, G. R., and SETAKA, M., 1973, *Molec. Crystals liq. Crystals,* **19**, 279.

[9] HUMPHRIES, R. L., and LUCKHURST, G. R., 1973, *Chem. Phys. Lett.,* **23**, 567.

[10] LUCKHURST, G. R., ROMANO, S., and SIMPSON, P., 1982, *Chem. Phys.,* **73**, 337.

[11] ZANNONI, C., 1979, *The Molecular Physics of Liquid Crystals,* edited by G. R. Luckhurst and G. W. Gray (Academic Press), Chap. 9.

[12] HASHIM, R., LUCKHURST, G. R., and ROMANO, S., 1985, *Molec. Phys.,* **56**, 1217.

[13] METROPOLIS, N., ROSENBLUTH, A. W., ROSENBLUTH, M. N., TELLER, A. H., and TELLER, E., 1953, *J. chem. Phys.,* **21**, 1087.

[14] BARKER, J. A., and WATTS, R. O., 1969, *Chem. Phys. Lett.,* **3**, 144.

[15] OWICKI, J. C., and SCHERAGA, H. A., 1977, *Chem. Phys. Lett.,* **47**, 600.

[16] VIEILLARD-BARON, J., 1974, *Molec. Phys.,* **28**, 809.

[17] FRENKEL, D., and EPPENGA, R., 1984, *Molec. Phys.,* **54**, 1303.

[18] LUCKHURST, G. R., and SIMPSON, P., 1982, *Molec. Phys.,* **47**, 251.

[19] JÄHNIG, F., 1981, *Biophys. J.,* **36**, 347.

[20] MARSH, D., 1985, *Progress in Protein–Lipid Interactions,* edited by A. Watts and J. J. H. M. de Pont (Elsevier Science Publishers), Chap. 4.

[21] SHENG, P., and WOJTOWICZ, P. J., 1976, *Phys. Rev.* A, **14**, 883. VAN DER HAEGEN, R., DEBRUYNE, J., LUYEKX, R., and LEKKERKERKER, H. N. W., 1980, *J. chem. Phys.,* **73**, 2469.

[22] FABER, T. E., 1980, *Proc. R. Soc.* A, **370**, 509.